공학석사 학위논문

Phase Behavior of Block Copolymers under Conical Confinement

원뿔 모양의 가둠 안에서의 블록공중합체의 상 거동

2018년 8월

서울대학교 대학원

화학생물공학부

황 성 열

Abstract

Constraints imposed by nanometer scaled confinement lead to the changes in bulk equilibrium behavior of block copolymers (BCPs). Especially, cylindrical pores with diameter corresponding to the equivalent length of several copolymer chains have been employed to investigate the influence of two-dimensional (2D) confinement on the behavior of BCPS. In this study, poly (styrene-*b*-butadiene) block copolymers was confined within conical pores and their morphologies are investigated using electron microscopy. Anodized aluminum oxide (AAO) templates with conical pores fabricated using multi-step anodization were used as confining matrix. On the basis of detailed observation, we demonstrated the effect of pore size, shape and surface energy on the phase behavior of block copolymers under conical confinement.

Keywords: Block copolymer, conical confinement, anodized aluminum oxide, phase behavior

Student number: 2015-21093

Contents

List of Tables

List of Figures

1. Introduction

Block copolymers (BCPs) has been widely studied due to their ability to generate self-organized periodic nanostructures over large scale. [1,2] BCPs consist of chemically distinct homopolymer chains covalently linked together at one end. Depending on the volume fraction of block chains, chain length and interaction parameter between polymer chains, different types of periodic nanostructures such as spheres, cylinders, lamellae and gyroids can be realized.

Because of the ability to feasibly fabricate nanoscale pattern, many studies have been done to engineer and control novel morphologies by utilizing external fields. Especially, template-assisted self-assembly was studied under a variety of geometry; 1D confinement such as thin film, 2D confinement using cylindrical channels or trenches, and 3D confinement. [3-11] The self-assembly of BCPs in 2D confined space is facile and robust technique to make new nanostructures which is not shown in bulk state. [12-14] Nanoscale hierarchical patterns using both intrinsic property of BCPs and topological templates can play a significant role in application such as optical sensors, photonic crystals and organic

devices. [15-17]

AAO templates were used to induce 2D confinement because of feasibility of fabrication and controlling the pore size. In cylindrically confined space, the degree of confinement is defined as the ratio of diameter of pores (D) and the copolymer chain's characteristic length (L_0). The self-assembly of BCPs in cylindrical confinement is mainly affected by two factors; intrinsic property of BCP chains such as interaction parameter, molecular weight and volume fraction and external factors such as interaction between surface, commensurability and curvature. By controlling these factors, novel morphologies of BCPs including torus, helix and peapod were identified. [18, 19]

In this study, we fabricated new type of AAO templates which have hexagonally arrayed conical pores. Nano- or microscale conical arrays are intriguing due to gradient profile and its corresponding optical and wetting properties. Also, the tapered diameter of cone geometry can induce distinctive effect on the conformation of polymer chains under confinement due to gradual change of the degree of confinement. As the cross-sectional diameter of conical pore is decreasing along the depth, the radius of curvature at vertex is eventually less than characteristic length of copolymer chains. In

this region, the loss of conformational entropy of polymer chains would be increasing and the phase behavior of block copolymers could be dominated by entropic factor.

To demonstrate the effect of geometry in thermodynamic perspective in detail, the size, shape and surface energy of the conical pores are controlled. On the basis of electron microscopic observation, we identified that the entropic penalty at the vertex, surface energy of pores and interfacial energy at the air surface comparatively influence the phase behavior of block copolymers under conical confinement.

2. Experimental Details

2.1. Materials

Lamellae forming Poly(styrene−*b*−1,4 butadiene) (SBD42, M_w/M_n=1.03) were purchased from polymer source, Inc., Canada. The repeat periods (L_0) of SBD42 was 30 nm. The high−purity aluminum foil (99.999%) was purchased from Good Fellow and used without any further purification. The perchloric acid, ethanol, oxalic acid and phosphoric acid were purchased from Sigma Aldrich.

2.2 Fabrication of AAO templates

We fabricated two types of conical AAO templates; one with large conical pore of diameter 225 nm and small conical pore with 80 nm diameter. To identify the effect of curvature at the vertex, AAO templates with truncated conical pore and cylindrical pore are prepared. These templates were fabricated by following procedure. (Figure 1) Detailed size of fabricated pore arrays are summarized on table 1.

2.2.1. Small sized conical AAO

The top diameter of small conical pore (D_p) was 80 nm. Conical pores of AAO templates were fabricated by the multi-step anodization process. [20-24] First, a high-purity aluminum foil was degreased in acetone and isopropanol solution. Subsequently, the aluminum slice (2x5 cm) was electropolished in a perchloric acid ($HClO_4$) and ethanol (C_2H_5OH) mixture (v/v=1:4) at 20 V. The polished aluminum sheet was then anodized at 40 V in 0.3 M oxalic acid solution maintained at 15 ℃ for 12 h. After the first anodization, the aluminum oxide layer was chemically removed by etching in an aqueous solution of phosphoric acid (6.8 wt %) and chromic acid (1.8 wt %) at 60 ℃ for 8 h.

To fabricate conical pore array, the chemically etched aluminum plate is alternatively anodized and pore widened. [23,24] In detail, the chemically etched aluminum plate is anodized in same electrolyte of 1^{st} anodization for a few second and pore widened in aqueous phosphoric acid solution at 30 ℃ for a few minute at each cycle, and the cycle is processed more than 12 times. The reaction time was varied to make different depth of pores; 160, 240 and 400 nm.

2.2.2. Small sized truncated conical AAO

We fabricated truncated small pore array which has larger bottom radius. First, conical pore with diameter of 60 nm was prepared and pores were widened to make top diameter as 80 nm. The bottom radius of truncated conical pore was 40 nm and the depth was consistent with conical pores.

2.2.3. Small sized cylindrical AAO

To fabricate cylindrical small pore array, second anodization was conducted at same condition for a few minute and pores were fully widened (80 nm). the depth was consistent with conical pores.

2.2.3. Large sized conical AAO

The diameter of pore (D_p) of large conical pore was 225 nm. The electropolished aluminum sheet was anodized at 112 V in 4wt % phosphoric acid solution maintained at 0 ℃ for 9 h to fabricate large pore array, followed by chemical etching to remove alumina layer. The large size conical pores were also fabricated by multi-step anodization. The process condition for the second anodization was same as that of smaller conical pore fabrication, but the time to reaction for anodization and pore-widening was longer.

Table 1. Detailed information of fabricated AAO pores.

	Diameter of pore (D_p)	Aspect Ratio (AR, height/D_p)	Radius of curvature (D_B)
Small Cone	80 nm	2, 3, 5	15 nm
Large Cone	225 nm	2, 3, 5	71 nm
Truncated Cone	80 nm	2, 3, 5	40 nm
Cylinder	80 nm	2, 3, 5	80 nm

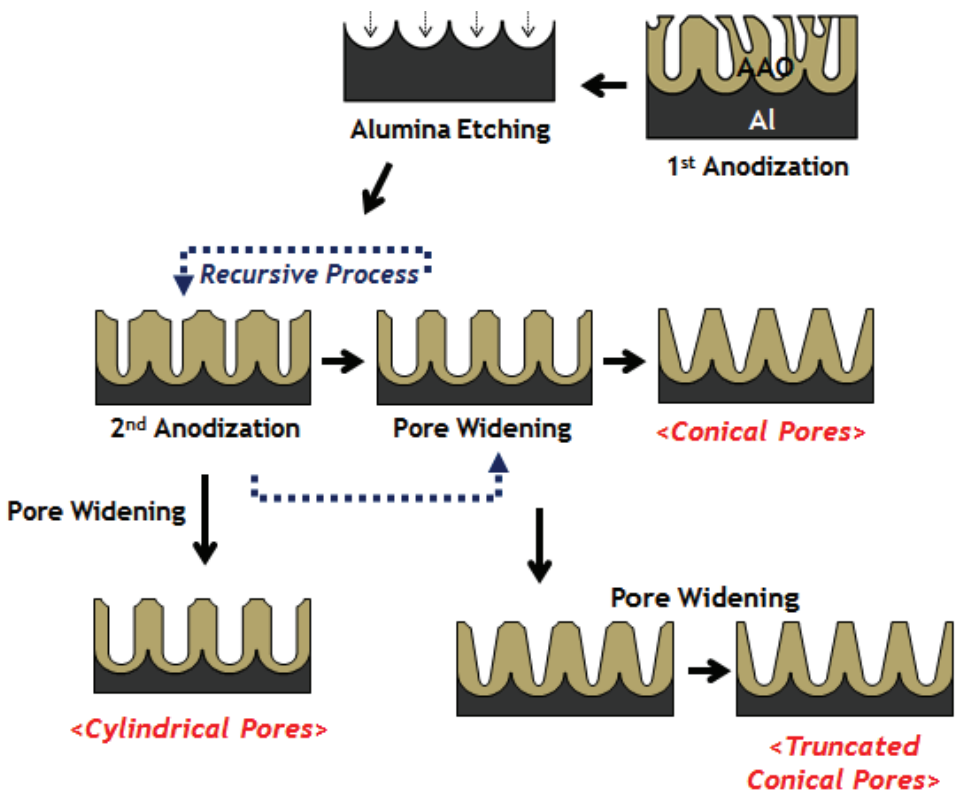

Figure 4. Process to fabricate conical, truncated conical and cylindrical pore array of AAO templates.

2.3. PS brush grafting on the surface of AAO

The surface energy of AAO wall were controlled by anchoring polystyrene brush on pore surface. The hydroxyl-terminated PS solution was spin-coated on porous AAO and it was annealed at 180 ℃ under vacuum for different time. Non-grafted polymer chains within the pore were completely removed by sonication in toluene. [25] The grafting density of PS-brush was dependent upon annealing time and consequently the wettability of PS block to the pore surface controlled by the grafting density of PS brushes.

2.4. PS-*b*-PBD inside AAO templates

SBD42 is spin-coated on fabricated AAO templates. Concentration of polymer solution and spin-rate were controlled to fill the pores but not overflow. After 24 hour drying in a vacuum. Samples were annealed under vacuum at 125 ℃ for 4 days. For PS brush grafting, the annealing time was varied from 20min to 120h. To prepare the sample for ultramicrotoming, aluminum layer and alumina were then removed in copper chloride ($CuCl_2$)/hydrochloric acid (HCl) solution and 5.0 wt % sodium hydroxide (NaOH) solution, respectively. Freestanding SBD nanocone arrays were embedded in

an epoxy resin composed of Embed 812, dodecenylsuccnic anhydride (DDSA), nadic methyl anhydride (NMA) and DMP-30 (Ted Pella). After curing at 60 ℃ for 48 h, the epoxy-embedded samples were sectioned with a diamond knife into ~70 nm thin pieces using a Leica Ultramicrotome. Prepare sample was stained in OsO_4 vapor for 1 hr to get enough contrast in microscopic observation.

2.5. Characterization

The geometries of AAO nanopores were analyzed with field emission Scanning electron microscope (FE-SEM, JSM- 6701F, JEOL) operated at an acceleration voltage of 10.0 kV. The morphologies of BCP nanostructures were characterized by a transmission electron microscope (TEM, JEM1010, JEOL) at 80.0 kV. PBD domains were selectively stained with aqueous OsO4 solution (2.0 wt %, Electron Microscopy Sciences) followed by TEM characterization.

3. Results and Discussion

The morphologies of SBD42 under conical confinement were investigated. Bottom geometries were controlled to vary the radius of curvature at the vertex. As the radius of curvature was increased, the pore shape was changed from cone to truncated cone and cylinder. We could identify the effect of entropic penalty at the vertex by altering the bottom geometry. The surface energy was also controlled by anchoring PS brushes on AAO surface to analyze the comparative effect of enthalpic and entropic factors on the phase behavior of block copolymers.

3.1. Pore size control

In order to demonstrate the effect of confining geometry, pore size including aspect ratio (AR) and pore diameter (D_p) was controlled. The diameter of small conical pore was 80 nm and the depth (h) was controlled to make the aspect ratio (h/D_P) 2, 3 and 5. (figure 2)

Similarly, large conical pore size was controlled by changing the aspect ratio and pore diameter. But the time ratio of anodization

and pore widening had to be different, because the solution of second anodization for small pore and large pore is identical and the dimension is 3 times larger than smaller one. So the template had to be anodized and pore widened to be the 2, 3 and 5 aspect ratio which is shown at figure 3.

As increasing the aspect ratio, we can alter the parameter of confinement gradient. The confinement gradient would decrease as increasing the aspect ratio. Also, the smaller dimension of conical pore would increase overall degree of confinement to BCPs and can make another nanostructure.

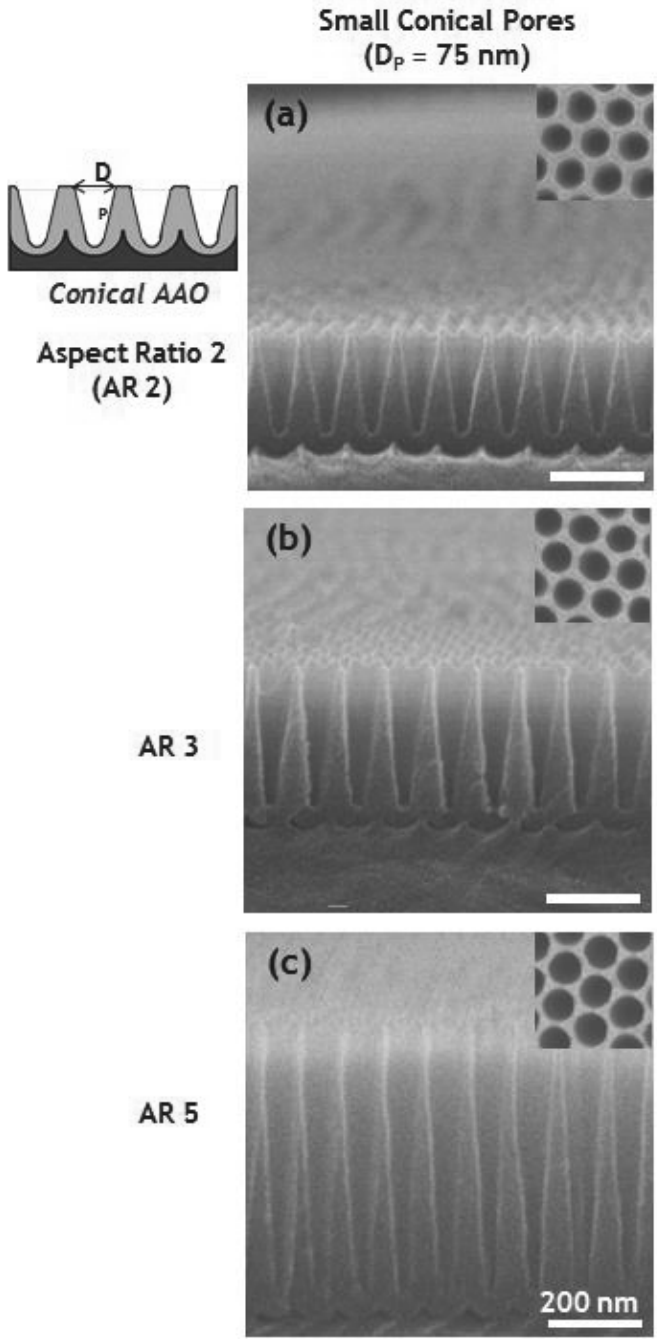

Figure 5. Cross section of small conical pore characterized by SEM. The small conical pore has (a) AR 2, (b) AR 3, (c) AR 5. Inset of the image is top view of AAO pores.

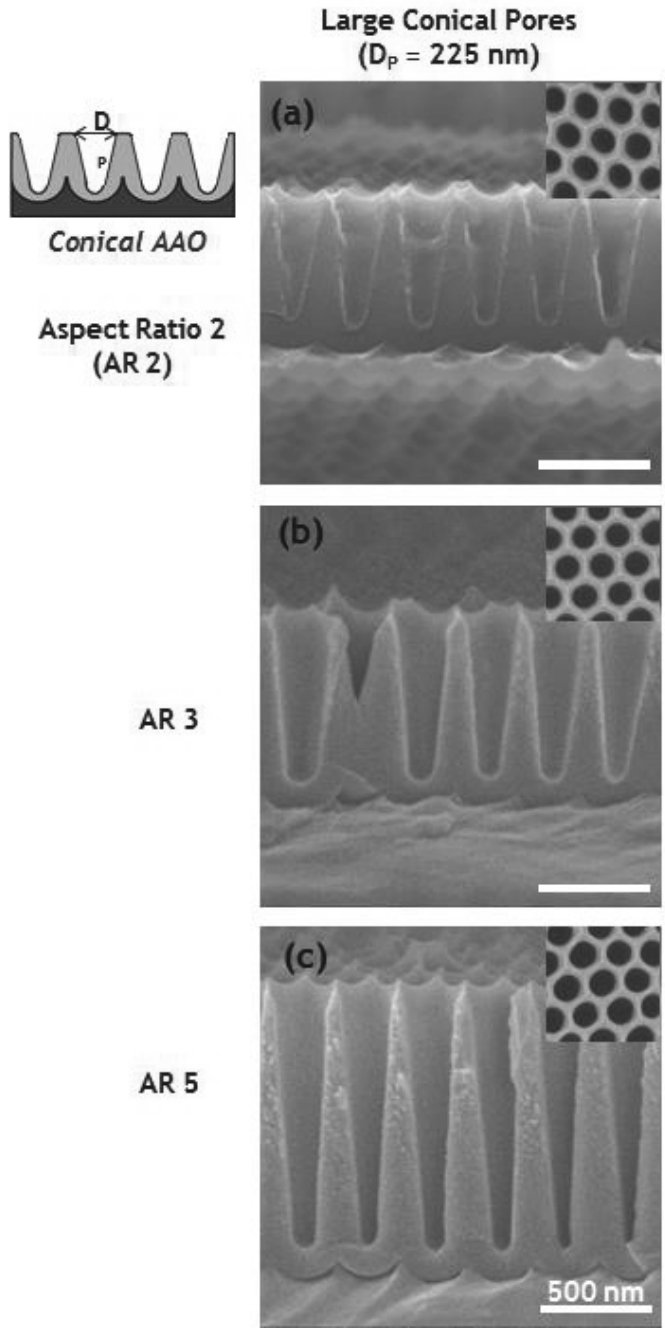

Figure 6. Cross section of large conical pore characterized by SEM. The large conical pore has (a) AR 2, (b) AR 3, (c) AR 5. Inset of the image is top view of AAO pores.

We investigated the nanostructure of SBD42 in small and large conical confinement varying the AR and D_p with TEM which is shown at figure 4.

At figure 4 (d), (e) and (f), BCPs are constrained under large conical confinement, and the copolymers have horizontally stacking morphology which is called lamellar stack at the surface of air-polymer. And the PBD chain wetted the AAO surface after the air-polymer surface induced lamellar stack. The effective distance of air-polymer surface is shown 3 L_0 (~90nm) which could be observed at figure 4. The effect of vertex is not shown because the scale of conical confinement is too large compared to the characteristic length of SBD 42.

At figure 4 (a), (b) and (c), BCPs are constrained under small conical confinement, and we also could observe the copolymers have lamellar stack at the surface of air-polymer. However, we found something different at the vertex of conical shape. Though the AAO surface is selective to PBD chain of SBD 42, the staking lamellar is formed at the vertex of conical shape. We think this morphology is formed because the entropy that polymer want to be vertically stacked overwhelmed the enthalpy that PBD want to be attached to AAO surface. In other words, the enthalpy is dominated by the

entropic penalty. The entropic penalty is formed due to the high degree of confinement at vertex. The degree of confinement (L_0/D) at the vertex is less the 1 and it would make no space to BCPs selectively be attached to the surface of AAO. And we call it ‘vertex effect’. Therefore, the stacked lamellar is formed all over the conical shape at figure 4 (a) and (b) of which the aspect ratio is 2 and 3 respectively.

However, there is strange morphology at the middle of the conical shape at figure 4 (c) of which the aspect ratio is 5. We think the entropic penalty at the vertex get weakened as going far from the vertex, and the air−polymer surface effect either get weakened as going far from the air surface. Therefore, increasing aspect ratio makes the area where the enthalpic term dominate the vertex entropic penalty and air surface effect. And the mix morphology is formed in that area. So we think the enthalpy would be similar or superior to the entropic penalty at the area where the mixed morphology is observed. And the vertex effect’s influence distance is considered about 3−4 L_0 (90−120nm), as we investigate the figure 4 (c).

Although we did not try further long aspect ratio of conical confinement, we expect that the morphology that PBD selectively wet

the surface of AAO would be formed if the aspect ratio is increased. Of course the transitional mixed morphology would be formed between the PBD enveloping morphology and staked lamellar.

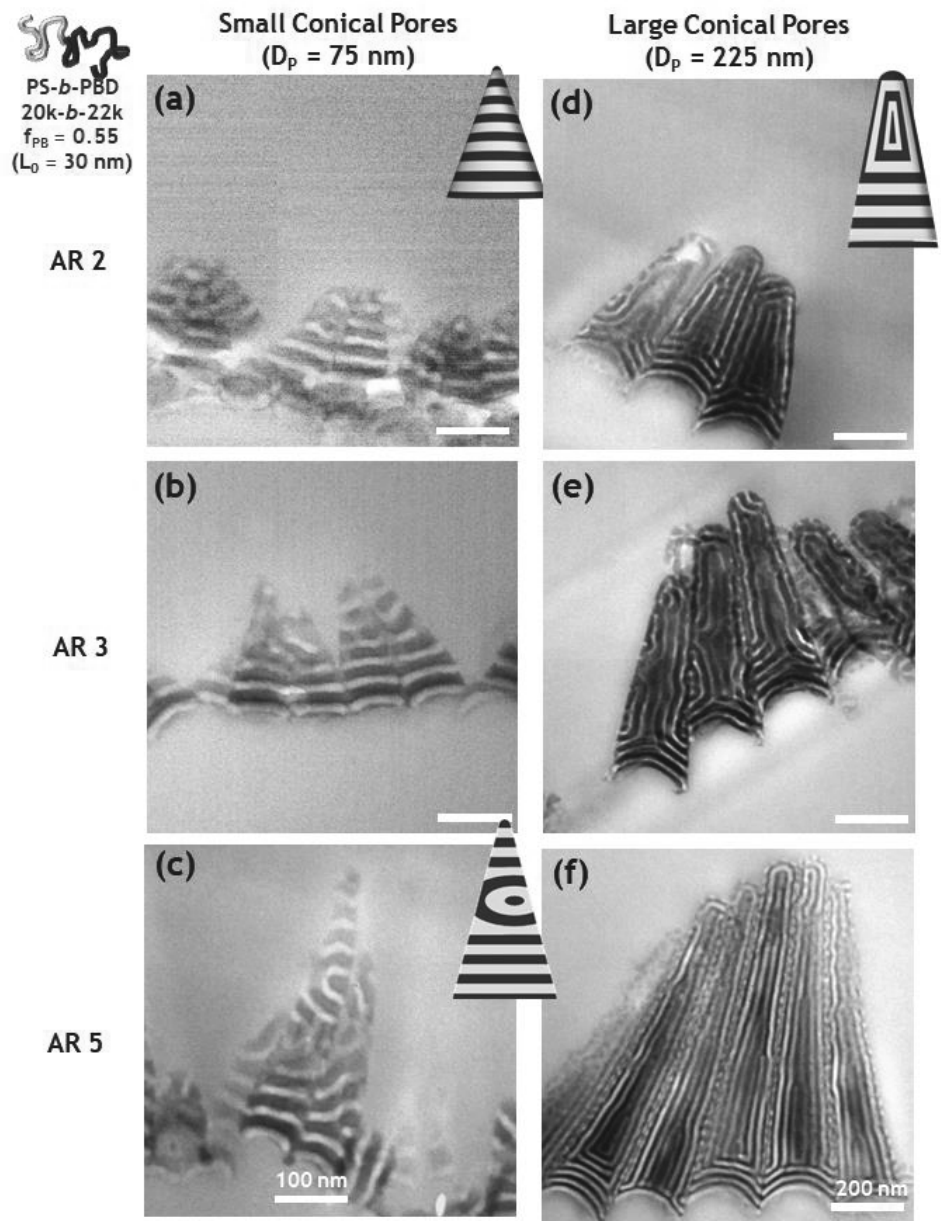

Figure 4. TEM images of SBD 42 in small and large conical confinement. SBD42 is confined in small conical confinement at (a) AR 2, (b) AR 3 and (c) AR 5. And SBD 42 is confined to large conical confinement at (d) AR 2, (e) AR 3 and (f) AR 5. The transitional phase is observed at (c).

3.2. Vertex geometry control

As we want to investigate the vertex effect, the vertex geometry is controlled altering radius of curvature at vertex. And the radius of curvature is measured as diameter at the vertex (D_B). The vertex effect would be decreased by increasing the radius of curvature at vertex. Therefore, we fabricated conical, truncated conical and cylindrical array, and the vertex effect would be decreased in order of cone, truncated cone and cylinder.

The truncated conical AAO is fabricated by pore widening the conical array. The pore diameter and the diameter at the vertex is increased from 70 nm to 83 nm and from 20 nm to 45 nm respectively as the template get pore widened and it is shown at figure 5. And the aspect ratio of fabricated truncated conical pore is 2, 3 and 5 which is shown at figure 6.

The Cylindrical AAO is fabricated by the transitional method to make cylindrical pore. And the height of the cylinder is adjusted by referring the graph of figure 7 (d). The fabricated cylindrical AAO is AR 2, 3 and 5 as shown at the figure 7.

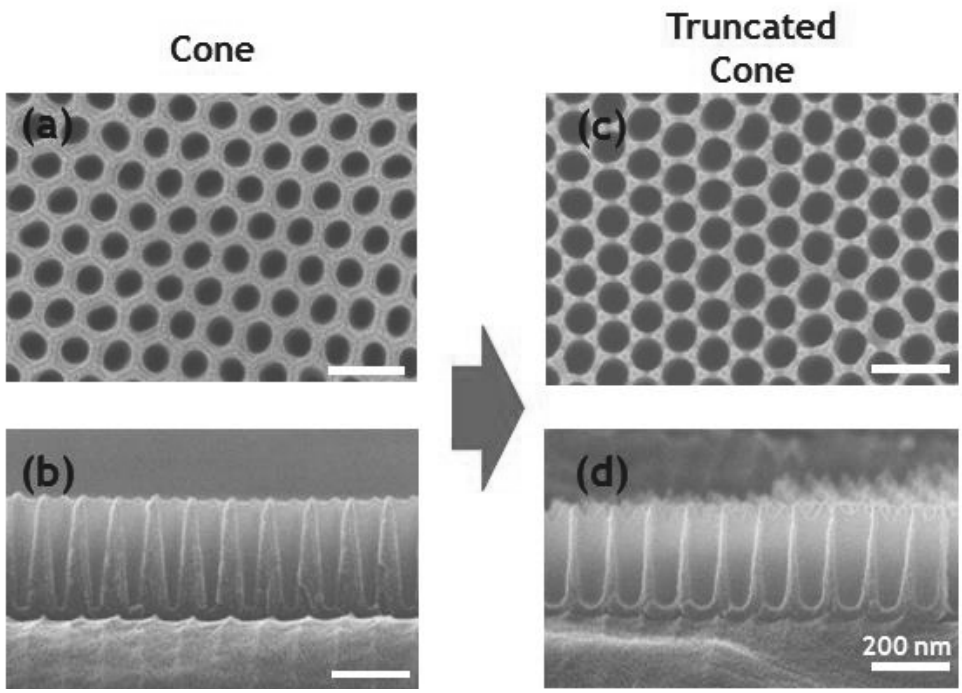

Figure 5. Pore widened truncated cone from conical array. (a) is the top view of the conical AAO and (b) is the cross section of conical AAO. And (c) and (d) truncated conical AAO which is pore widened from (a) and (b). The cross section of truncated conical AAO is (d) and the top view is (c). The pore diameter and the diameter at the vertex is increased from 70 nm to 83 nm and from 20 nm to 45 nm respectively as the template get pore widened.

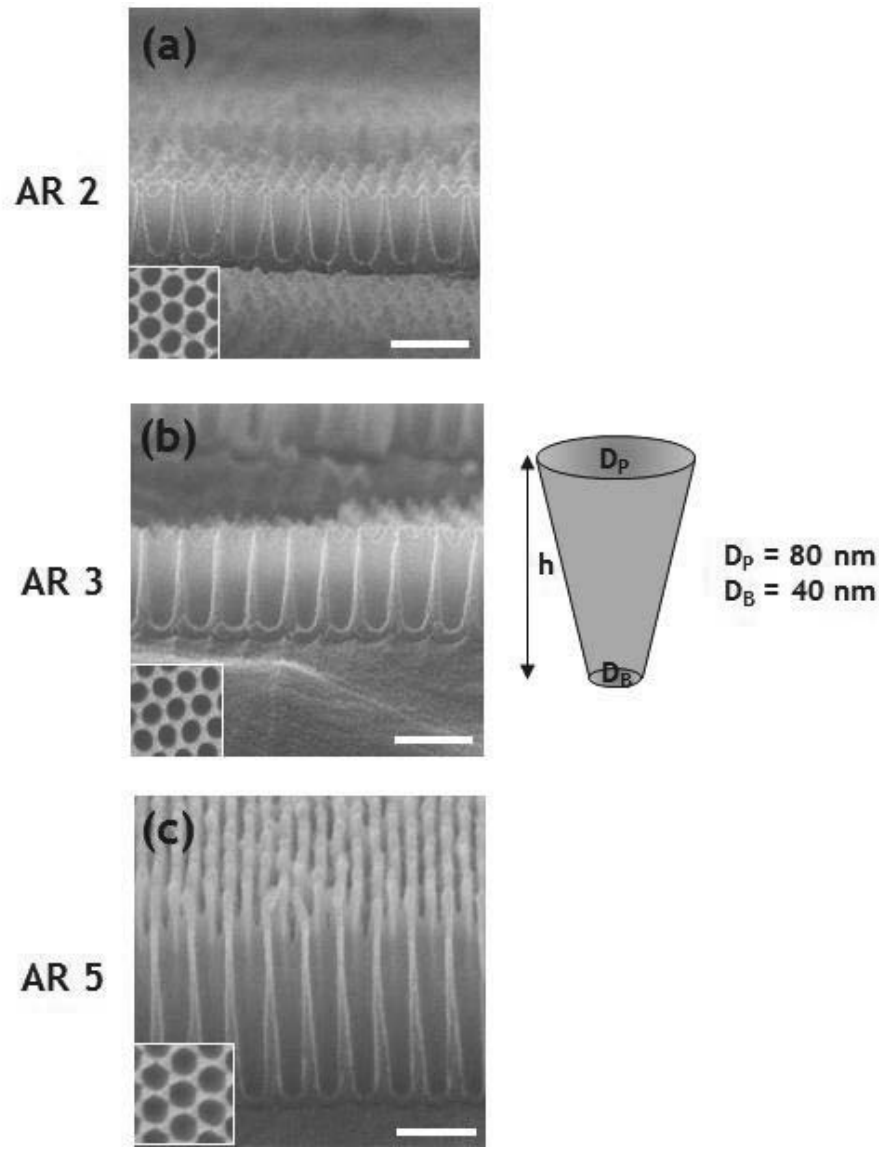

Figure 6. The cross section SEM image of truncated conical AAO. The aspect ratio of truncated cone is (a) 2, (b) 3, and (c) 5. And the diameter at the pore entrance and vertex is 40 nm and 80 nm respectively.

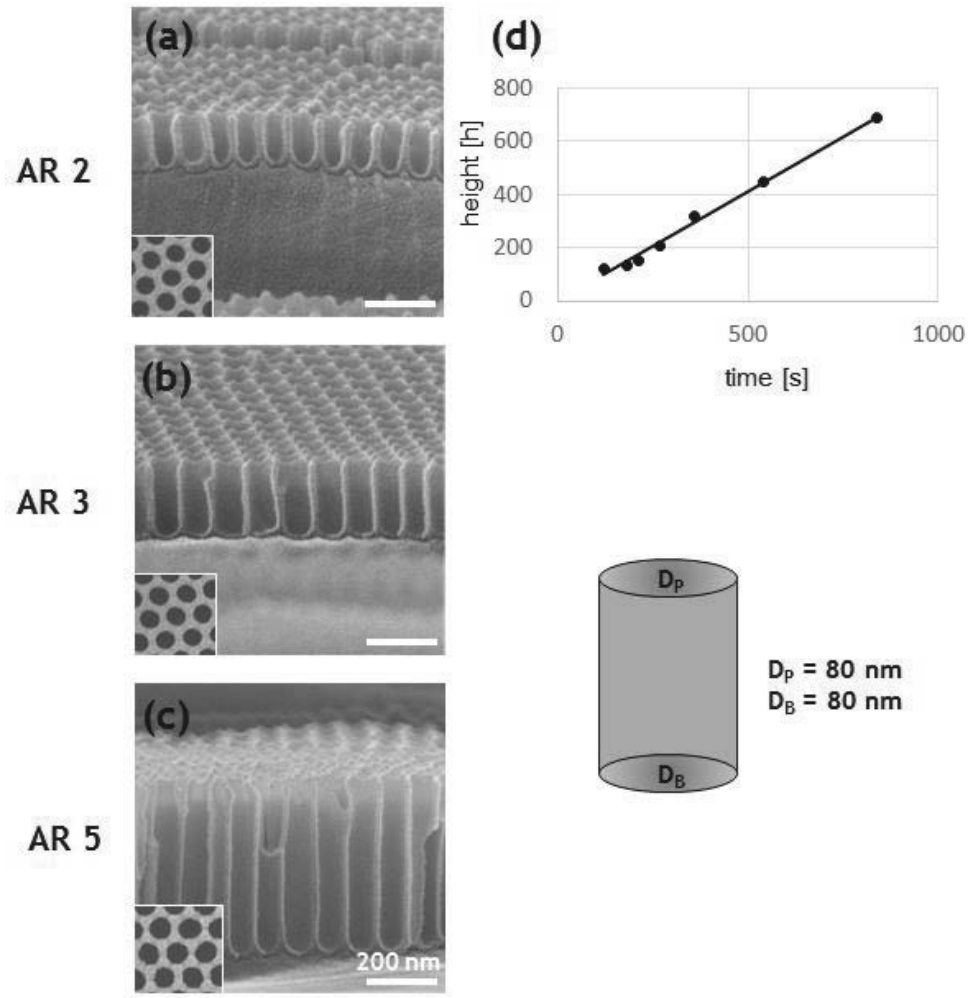

Figure 7. The cross section SEM image of cylindrical AAO and the graph of the relation of height and anodizing time. The aspect ratio of cylindrical AAO is (a) 2, (b) 3 and (c) 5. And the graph of relation with height of cylindrical AAO and anodizing time is (d).

We investigated the nanostructure of SBD44 in conical, truncated conical, cylindrical confinement and the TEM images are shown at figure 8. As the D_B increases, the entropic penalty at the vertex would be decreased and the enthalpy would easily dominate the enthalpy which is from the interfacial energy between PBD chains of BCPs and the surface of AAO. The schematic figure of BCP chains under the conical, truncated conical and cylindrical confinement is shown at figure 9.

The figure 8 can be interpreted that the decreased vertex effect makes the magnitude of the entropic penalty weakened, as the transitional mixed morphology is formed earlier by increasing the radius of curvature at the vertex. The mixed morphology is formed at the AR 5 under the conical confinement, and at the AR 3 under the truncated conical confinement, and at the AR 2 under the cylindrical confinement. The images in the red box at the figure 8 are the images where the transitional phase is observed. And the polymer-air surface effect is still about 3-4 L_0.

Under the truncated conical confinement whose D_B is 45 nm, the effective range of the vertex effect seems about 1-2 L_0 (30-60 nm). It can be observed at figure 8 (d), (e) and (f). One or two white lamellar line of PS component exist at the vertex of cone at figure 8

(e) and (f). Moreover, the 5 white line is observed at figure 8 (d), which means that the range of vertex effect is 1−2 L_0, because the effective range of polymer−air surface interfacial energy is about 3−4 L_0.

The vertex effect under the cylindrical confinement seems zero, because there is no stacked lamellar at the tip of cylinder at figure 8 (g), (h) and (i). At figure (i), the transitional morphology is not formed and only the concentric ring morphology and polymer−air interfacial energy effect exist.

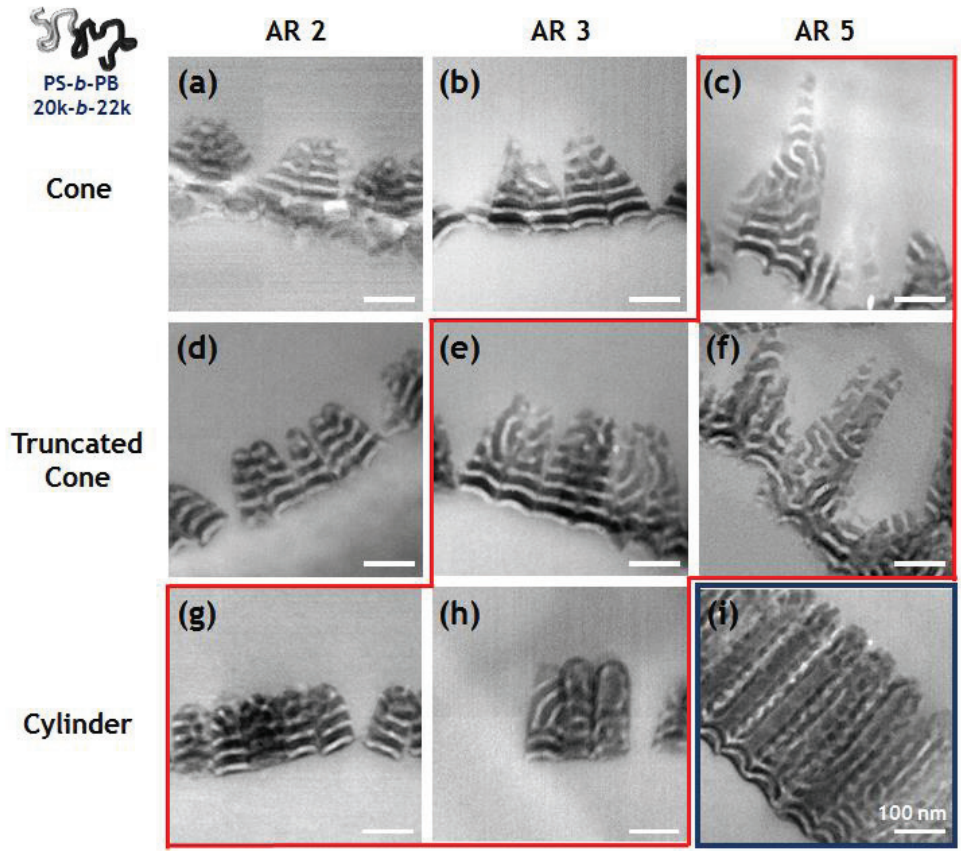

Figure 8. TEM images of SBD42 in conical, truncated conical and cylindrical confinement. SBD 42 is confined in conical confinement at (a) AR 2, (b) AR 3 and (c) AR5. SBD 42 is confined in truncated conical confinement at (d) AR 2, (e) AR 3 and (f) AR 5. SBD 42 is confined in cylindrical confinement at (g) AR 2, (h) AR 3 and (i)AR 5. The transitional mixed morphology is observed in the red box.

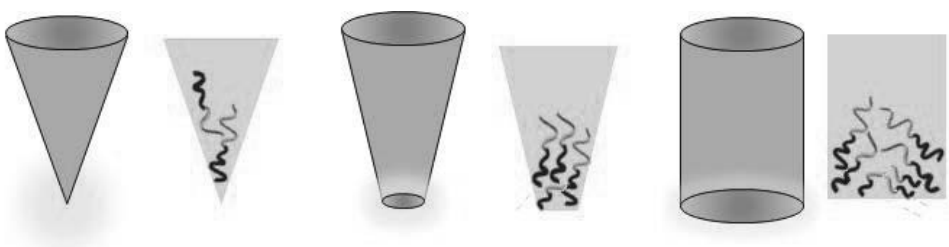

Figure 9. Scheme of BCP chains under the conical, truncated conical and cylindrical confinement.

3.3. Surface selectivity of AAO

In nature, the AAO selectively prefer the PBD chain than PS chain. However, we attached PS graft on AAO surface and investigated the SBD42 morphology by increasing the PS brush density. The increased PS brush density means increased selectivity to PS chain. The PS brush density can be controlled by altering the annealing time of AAO with PS-OH. The morphology of SBD42 with increasing PS brush density is shown at figure 10. As the PS brush density increases, the magnitude of enthalpy to attach PS chain to surface of AAO increases. Thus there at the 120hr annealing, PS chains are perfectly coated to the surface of AAO which means enthalpy overwhelmed the entropy. It is observed that annealing time less than 48hr makes not enough enthalpy to overwhelm the entropy, and transitional phase is observed.

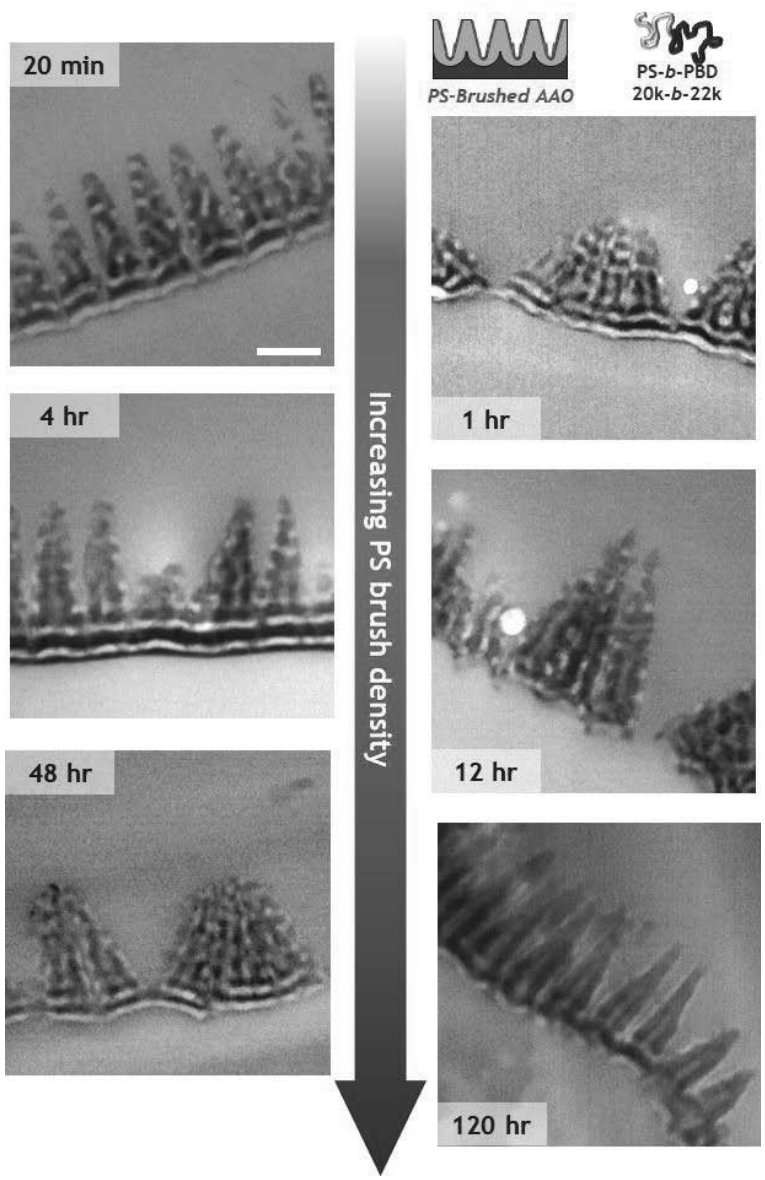

Figure 10. TEM imaged of SBD42 in small conical confinement with PS selective AAO surface. The annealing time of AAO with PS-OH is 20min, 1hr, 4hr, 12hr, 48hr, 120hr. As the annealing time increases, the PS brush density also increases.

4. Conclusion

In this study, we fabricated various type of conical pores which have different pore size, bottom geometry and surface selectivity to investigate the effect of pore geometry. We proved that the entropic penalty at the vertex can make vertically stacked lamellae morphology and its morphology is mainly influenced by the radius of curvature at vertex. As the surface energy of AAO surface is changed to PS-wetting, however, the morphology of BCPs are transited to concentric conical morphology. In thermodynamic view, it means that energetic factor dominated the entropic factor in phase behavior of BCPs under confinement.

Controlled morphologies of BCPs nanocone array can be used in optical application such as anti-reflective coating in broadband wavelength. Since conical array can also have superhydrophobic wetting property, it can be utilized in the solar cell panel to absorb more solar energy per area by decreasing the reflected solar energy. [26, 27]

References

1. A. K. Khandpur, S. Foerster, F. S. Bates, I. W. Hamley, A. J. Ryan, W. Bras, K. Almdal, and K. Mortensen, *Macromolecules*, **28**, 8796 (1995).

2. M. W. Matsen and F. S. Bates, *Macromolecules*, **29**, 1091 (1996).

3. R. J. Albalak and E. L. Thomas, *J. Polym. Sci. Part B: Polym. Phys.*,**32**, 341 (1994).

4. P. W. Majewski, M. Gopinadhan, and C. O. Osuji, *J. Polym. Sci. Part B: Polym. Phys.* **50**, 2 (2012).

5. J. Y. Cheng, A. M. Mayes, and C. A. Ross, *Nat. Mater.*, **3**, 823 (2004).

6. S. H. Kim, M. J. Misner, T. Xu, M. Kimura, and T. P. Russell, *Adv. Mater.*, **16**, 226 (2004).

7. P. Mansky, T. P. Russell, C. J. Hawker, M. Pitsikalis, and J. Mays, *Macromolecules*, **30**, 6810 (1997).

8. R. A. Segalman, H. Yokoyama, and E. J. Kramer, *Adv. Mater.*, **13**, 1152 (2001).

9. H. S. Suh, H. Kang, C.-C. Liu, P. F. Nealey, and K. Char, *Macromolecules*, **43**, 461 (2010).

10. X. M. Yang, R. D. Peters, P. F. Nealey, H. H. Solak, and F. Cerrina, *Macromolecules*, **33**, 9575 (2000).

11. H.Yabu, T. Higuchi, H. Jinnai, *Soft Matter, **10**, 2919-2931* (2014).

12. P. Dobriyal, H. Xiang, M. Kazuyuki, J.-T. Chen, H. Jinnai, and T. P. Russell, *Macromolecules*, **42**, 9082 (2009).

13. K. Shin, H. Xiang, S. I. Moon, T. Kim, T. J. McCarthy, and T. P. Russell, *Science*, **306**, 76 (2004).

14. Y. Sun, M. Steinhart, D. Zschech, R. Adhikari, G. H. Michler, and U. Gösele, *Macromol. Rapid Commun.*, **26**, 369 (2005).

15. K. M. Coakley and M. D. McGehee, *Appl. Phys. Lett.*, **83**, 3380 (2003).

16. Y. Kang, J. J. Walish, T. Gorishnyy, and E. L. Thomas, *Nat. Mater.*, **6**, 957 (2007).

17. C. Park, J. Yoon, and E. L. Thomas, *Polymer*, **44**, 6725 (2003).

18. B. Yu, Q. Jin, D. Ding, B. Li, and A.-C. Shi, *Macromolecules*, **41**, 4042 (2008).

19. B. Yu, P. Sun, T. Chen, Q. Jin, D. Ding, B. Li, and A.-C. Shi, *Phys. Rev. Lett.*, **96**, 138306 (2006).

20. M. P. Stoykovich, E. W. Edwards, H. H. Solak, and P. F. Nealey, *Phys. Rev. Lett.*, **97**, 147802 (2006).

21. M. P. Stoykovich, M. Muller, S. O. Kim, H. H. Solak, E. W. Edwards, J. J. de Pablo, and P. F. Nealey, *Science*, **308**, 1442 (2005).

22. J. Xu, Y. Yang, K. Wang, J. Li, H. Zhou, X. Xie, and J. Zhu, *Langmuir*, **31**, 10975 (2015).

23. Y. Yamauchi, T. Nagaura, A. Ishikawa, T. Chikyow, and S. Inoue*, J. Am. Chem. Soc.*, **130**, 10165 (2008)

24. N. Nagaura, F. Takeuchi, Y. Yamauchi, K. Wada, and S. Inoue, *Electrochem. Commun.* **10**, 681 (2008)

25. D. Lee, M. Kim, D. Bae, JK Kim, Macromolecules, **47**, 3997-4003 (2014).

26. J. Zhu, C. Hsu, Z. Tu, S. Fan and Y. Cui, *Nano Letters*, **10**, 1979-1984 (2010).

27. Eyderman, S. John, and A. Deinega, *J. App. Phys.,* **113**, 154315 (2013).

국문 초록

황 성 열 (Sungyoul Hwang)

화학생물공학부

(School of Chemical & Biological Engineering)

The Graduate School

Seoul National University

블록공중합체의 자가조립 특성은 쉽고 빠르게 나노 스케일의 패턴을 만들 수 있기 때문에 이전부터 많은 연구가 이루어졌다. 특히 블록공중합체와 비슷한 크기 정도의 반지름을 가지는 원기둥에 2차원적으로 블록공중합체를 가두었을 때의 새로운 상 거동에 대한 연구가 많았다. 여기서 발전하여, 이 연구에서는 블록공중합체를 원뿔 모양과 끝이 뭉뚝한 원뿔 모양에 가두었을 때 나타나는 상 거동을 관찰하였다. 이때 사용한 틀은 본 연구실에서 다단계 양극 산화를 통해 만들어낸 원뿔 모양과 뭉뚝한 원뿔 모양의 기공을 가지는 산화 알루미늄 틀이다. 본 연구에서는 기공의 반지름, 기공의 높이, 기공의 형태, 기공의 표면 에너지를 바꾸면서 이에 따른 영향을 분석했다. 블록공중합체를 이 틀에 가둠으로써, 원뿔의 꼭지점에서 한쪽 사슬에 대해 선택적인 엔탈피의 힘을 이기며 사슬을 수직으로 서게 만드는

엔트로피를 관찰 할 수 있었다. 따라서 원뿔의 꼭지점 효과와 공기와 고분자가의 표면 에너지에 의한 효과에서는, 고분자가 수직으로 쌓여있는 형상을 관찰 할 수 있었고 그 사이에서는 과도기의 형상을 관찰 할 수 있었다.

주요어: 블록공중합체, 원뿔 가둠, 다단계 양극 산화된 산화알루미늄, 상거동

학번 : 2015-21093